



## Selective brain neuronal and glial losses without changes in GFAP immunoreactivity: Young versus mature adult Wistar rats



Leonardo D. Diene<sup>a</sup>, Zaquer S.M. Costa-Ferro<sup>b</sup>, Silvia Barbosa<sup>c</sup>, Bruna Bueno Milanese<sup>a</sup>, Gabriele Zenato Lazzari<sup>a</sup>, Laura Tartari Neves<sup>a</sup>, Lisiê Valéria Paz<sup>a</sup>, Paula Fernanda Ribas Neves<sup>a</sup>, Vanessa Battisti<sup>a</sup>, Lucas A. Martins<sup>a</sup>, Gunther Gehlen<sup>d</sup>, Régis Gemerasca Mestriner<sup>a</sup>, Jaderson C. Da Costa<sup>b</sup>, Léder L. Xavier<sup>a,\*</sup>

<sup>a</sup> Laboratório de Biologia Celular e Tecidual, Escola de Ciências da Saúde, Pontifícia Universidade Católica do Rio Grande do Sul, Porto Alegre, RS, Brazil

<sup>b</sup> Instituto do Cérebro do Rio Grande do Sul (InsCer/RS), Porto Alegre, RS, Brazil

<sup>c</sup> Laboratório de Histofisiologia Comparada, Instituto de Ciências Básicas da Saúde, Universidade Federal do Rio Grande do Sul, Porto Alegre, RS, Brazil

<sup>d</sup> Universidade Feevale, Novo Hamburgo, RS, Brazil

### ARTICLE INFO

#### Keywords:

Glia  
Neurons  
Astrocytes  
Ageing  
GFAP

### ABSTRACT

Normal ageing results in brain selective neuronal and glial losses. In the present study we analyze neuronal and glial changes in Wistar rats at two different ages, 45 days (young) and 420 days (mature adult), using Nissl staining and glial fibrillary acidic protein (GFAP) immunohistochemistry associated to the Sholl analysis. Comparing mature adults with young rats we noted the former present a decrease in neuronal density in the cerebral cortex, corpus callosum, pyriform cortex, L.D.D.M., L.D.V.L., central medial thalamic nucleus and *zona incerta*. A decrease in glial density was found in the dorsomedial and ventromedial hypothalamic nuclei. Additionally, the neuron/glia ratio was reduced in the central medial thalamic nucleus and increased in the habenula. No changes were found in the neuronal and glial densities or neuron/glia ratio in the other studied regions. The number of astrocytic primary processes and the number of intersections counted in the Sholl analysis presented no significant difference in any of the studied regions. Overall, neither GFAP positive astrocytic density nor GFAP immunoreactivity showed alteration.

### 1. Introduction

In humans and rodents, cognitive decline, memory loss and reduced learning ability are associated with brain ageing and losses of neuronal and glial cells throughout life, although in most cases there is no apparent major pathological component, in part, due to the action of healthy glial cells in protecting neurons and repairing damaged tissue in the central nervous system (CNS) (Chung et al., 2009; Tansey and Goldberg, 2010; Fabricius et al., 2013; Chinta et al., 2014; Lopez-Leon et al., 2014; Kalia and Lang, 2015; Ojo et al., 2015; Rodríguez-Arellano et al., 2016; Bellaver et al., 2016).

Among the glial cells, astrocytes are the most numerous in the brain (Pekny and Pekna, 2004), comprising as much as 25% of the cells and 35% of the total mass of the CNS (Eng et al., 1992). They perform key roles in normal brain physiology, including blood flow regulation, providing glucose and lactate to neurons, participating in synaptic function and plasticity, and maintaining the extracellular balance of

ions and fluids (Giaume et al., 2007; Rodríguez et al., 2009; Verkhratsky et al., 2012; Sofroniew and Vinters, 2010; Gomes et al., 2013). During the ageing process, astrocytes may react differently (through hyperplasia and/or reactive astrogliosis) in different brain regions, such as the striatum and the frontal cortex (Mythri et al., 2011; Eddleston and Mucke, 1993). Whilst there is no consensus regarding astrocytic density in humans, one study showed the number of astrocytes remains unchanged even in centenarian individuals (Fabricius et al., 2013).

By contrast, a previous study in rats showed the number of astrocytes and pericytes tends to increase by 20% in the cerebral cortex and other brain regions during ageing, while the number of oligodendrocytes and microglia remains unchanged (Cotrina and Nedergaard, 2002).

Ageing is also associated with increased glial fibrillary acidic protein (GFAP) expression. GFAP is a reliable astrocytic marker and increased GFAP immunoreaction is generally accepted as a sign of

\* Corresponding author at: 6681 Ipiranga Avenue, Porto Alegre, RS, 90619-900, Brazil.

E-mail address: [llxavier@pucrs.br](mailto:llxavier@pucrs.br) (L.L. Xavier).

<https://doi.org/10.1016/j.mad.2019.111128>

Received 25 March 2019; Received in revised form 18 July 2019; Accepted 6 August 2019

Available online 09 August 2019

0047-6374/ © 2019 Elsevier B.V. All rights reserved.

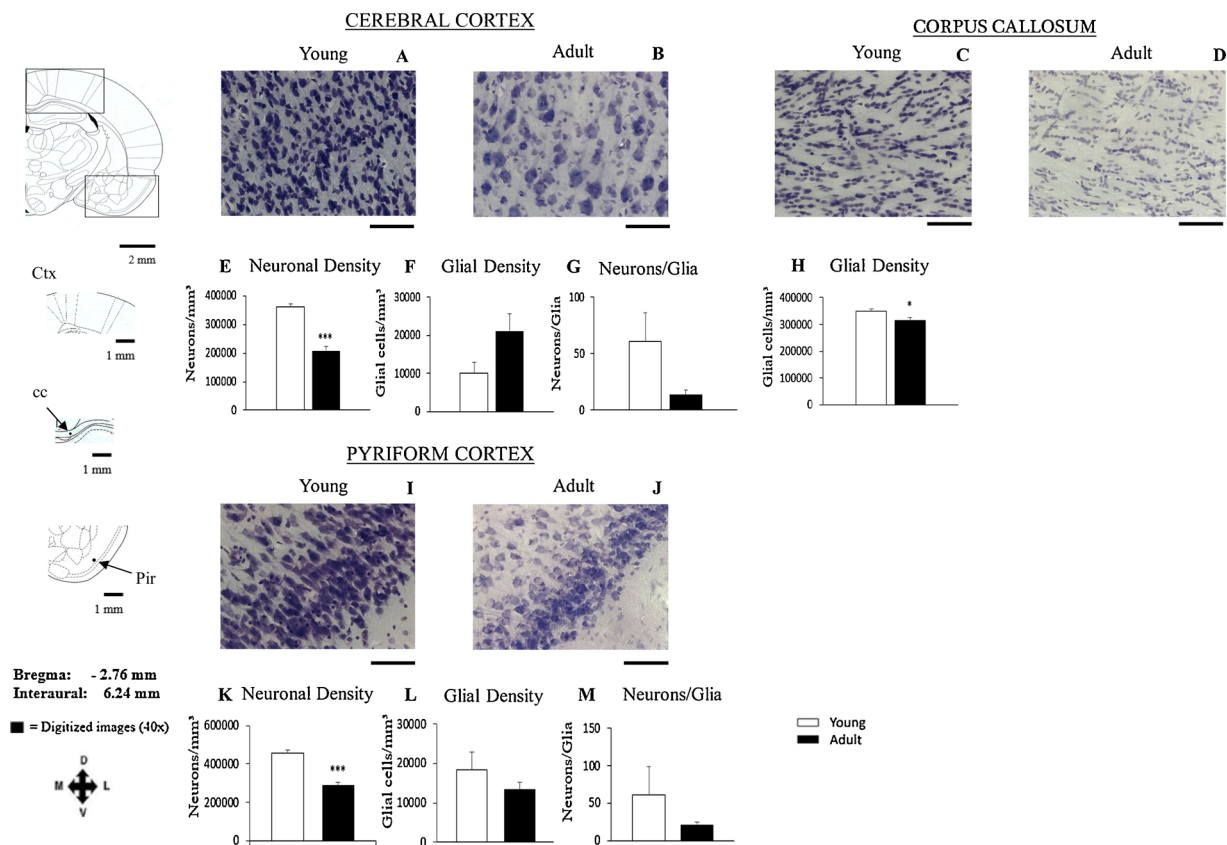


**Fig. 1.** Digitized images of coronal brain sections stained with Nissl showing the Cerebral cortex (Ctx) (A, B, E, F, G), Corpus Callosum (CC) (C, D, H) and Piriform Cortex (Pir) (I, J, K, L, M) in young and mature adult male Wistar rats. The following parameters are presented: Neuronal density (neurons/mm<sup>3</sup>) (E, K) Glial Cell density (glia/mm<sup>3</sup>) (F, H, L) and Neuron/Glia ratio (Neuronal density/ Glial Cell density) (G, M). Note 1 - No neurons were found in the corpus callosum, hence the neuron/glia ratio was zero, so it was not included in the figure. Note 2 - Only brain regions with significant morphological differences and/or relevant changes in GFAP immunoreactivity are presented in the figure, see Table 2. The schematic drawings were adapted from Paxinos and Watson's atlas (Paxinos and Watson, 2014) (Calibration bars = 100  $\mu$ m) (\*P < 0.05; \*\*\*P < 0.001).

pathological astroglial response (Cotrina and Nedergaard, 2002; Kohama et al., 1995; Nichols, 1999; Middeldorp and Hol, 2011). Astrogliosis, characterized by increased GFAP, is essentially a defensive reaction, represented by a complex continuum of morphological and functional remodeling of astroglia in the damaged brain region, aiding neuronal survival and regenerating the neuronal network (Rodriguez et al., 2013; Seifert et al., 2006). In its extreme form, reactive astrogliosis can lead to astrocytic proliferation and scar formation in response to tissue damage following trauma, stroke, infection, autoimmune responses or degenerative disease (Menet et al., 2001; Sofroniew, 2009; Sofroniew and Vinters, 2010; Jyothia et al., 2015). However, there is no consensus regarding age-dependent changes in astrocytic reactivity, as reflected by divergent results reported in previous studies (Unger, 1998; Lynch et al., 2010; Rodríguez-Arellano et al., 2016).

Thus, in the present study we have sought to analyze changes in neuronal and glial density using Nissl staining and evaluate GFAP immunoreactivity in Wistar rats at two ages: 45 days (young) and 420 days (mature adult).

## 2. Materials and methods

### 2.1. Animals

The animals were obtained from the *Centro de Modelos Biológicos Experimentais of the Pontifícia Universidade Católica do Rio Grande do Sul* and maintained in controlled environmental conditions with food and water *ad libitum*, under a 12/12h dark/light schedule. The twelve

healthy male Wistar rats were divided into 2 groups, 6 animals per group: the young group at 45 days old (1.5 months old, equivalent to 3 human years), weighing about 200 g; and the mature adult group at 420 days old (14 months old, equivalent to 30 human years) (Andreollo et al., 2012; Sengupta, 2013), weighing about 500 g. All experiments were performed in accordance with the Guide for the Care and Use of Laboratory Animals adopted by the National Institute of Health (USA). All efforts were made to minimize animal suffering and reduce the number of animals needed.

### 2.2. Brain regions analyzed

Since the rat brain is composed of approximately 1000 regions (Paxinos and Watson, 2014), in this study we decided to analyze the regions showing the most pronounced GFAP immunoreactivity located in the middle of the brain in the anterior-posterior axis, between Bregma -1.80 / Interaural 7.20 mm and Bregma -4.44 mm, Interaural 4.56 mm. This part of the brain includes important parts of the cerebral cortex, the anterodorsal hippocampus, dentate gyrus and many thalamic and hypothalamic nuclei.

The brain regions with the most pronounced GFAP immunoreactivity were defined based on a qualitative evaluation performed by two experts in neurohistology. In fact, all the other regions located between these Bregma/Interaural coordinates present very weak or no GFAP immunoreaction.

Thus, twelve brain regions were analyzed: five in telencephalon (1-cerebral cortex; 2-piriform cortex; 3-dentate gyrus; 4-corpor callosum and 5-hippocampus); five in thalamus (1-L.D.D.M.; 2- L.D.V.L.; 3-

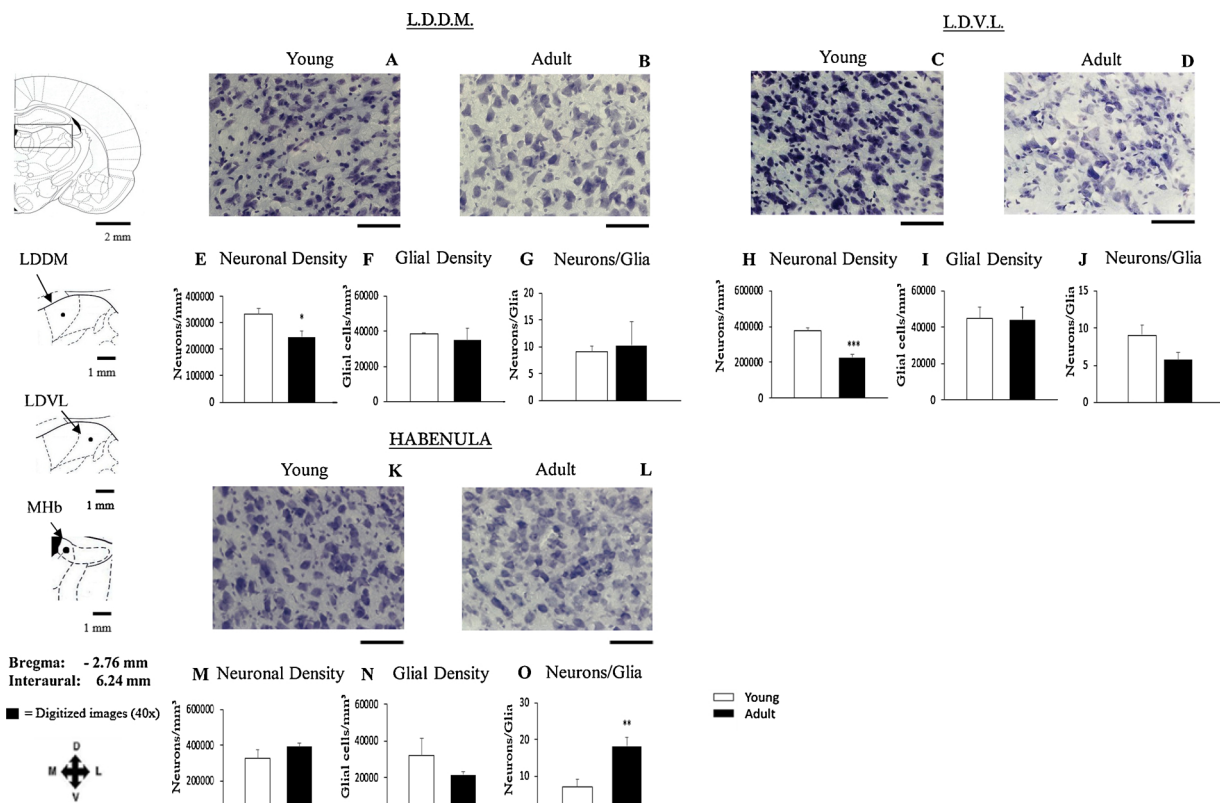


**Fig. 2.** Digitized images of coronal brain sections stained with Nissl showing the nucleus lateralis dorsale pars dorsomedialis (L.D.D.M.) (A, B, E, F, G), nucleus lateralis dorsale pars ventrolateralis (L.D.V.L.) (C, D, H, I, J) and Habenula (MHb) (K, L, M, N, O) in young and mature adult male Wistar rats. The following parameters are presented: Neuronal density (neurons/mm<sup>3</sup>) (E, H, M) Glial Cell density (glia/mm<sup>3</sup>) (F, I, N) and Neuron/Glia ratio (Neuronal density/ Glial Cell density) (G, J, O). Note that only brain regions with significant morphological differences and/or relevant changes in GFAP immunoreactivity are presented in the figures, see [Table 1](#). The schematic drawings were adapted from Paxinos and Watson's atlas ([Paxinos and Watson, 2014](#)) (Calibration bars = 100  $\mu$ m) (\* $P < 0.005$ ; \*\* $P < 0.01$ ; \*\*\* $P < 0.001$ ).

habenula; 4- central medial thalamic nucleus; 5- zona incerta) and two in hypothalamus (1-dorsomedial hypothalamic nucleus and 2-ventromedial hypothalamic nucleus).

### 2.3. Histological and immunohistochemical procedures

For the histological and immunohistochemical evaluation, all animals were deeply anesthetized with sodium thiopental (50 mg/kg, i.p.) and injected with 1000 IU of heparin. Thereafter, they were transcatheterially perfused through the left cardiac ventricle using a peristaltic pump (20 mL/min) with 200 ml of saline solution followed by 200 ml of 4% paraformaldehyde in 0.1 M phosphate buffer pH 7.2.

Brains were dissected from the skull, post-fixed for 4 h in the same fixative solution at room temperature, cryoprotected by immersion in 30% sucrose solution in PB at 4 °C until they sank (about 24 h). After these procedures, the brains were quickly frozen in liquid nitrogen. Coronal brain sections (50  $\mu$ m) were obtained using a cryostat Leica, Germany (CM1850) along the entire rostral-caudal axis. The sections are divided as follows, in accordance with their processing: 1-Nissl; 2-GFAP.

### 2.4. Nissl staining

For the Nissl (cresyl violet) staining method, sections were mounted on gelatin-coated slides and air-dried for 24 h to ensure adhesion. Thereafter, sections were rehydrated and stained with 0.1% cresyl violet solution at 36 °C for 6 min in acetate buffer. Soon after, the sections were dehydrated in 100% alcohol; bleached in toluol, coated with Dammar resin (Merck) and coverslipped.

### 2.5. Nissl-stained neuronal and glial density estimation

The stereological estimation of neuronal and glial cell densities was performed using Olympus BX51 microscope with a CCD camera coupled (Qimaging, model MicroPublisher 3.3 RTV). The selected images were analyzed with the aid of Image Pro Plus software 6.0 (Media Cybernetics USA).

Firstly, the morphological distinction of neurons and glia cells was performed - the neurons were identified by their large, pale nuclei surrounded by dark cytoplasm containing Nissl bodies, while the glial cells were identified by their relative size to the neurons and lack of stained cytoplasm. The nucleoli and nuclei were used as the counting marker for neurons and glia, respectively.

The neuronal and glial cell densities were estimated using an adaptation of the dissector and fractionator methods ([Stereo, 1984](#); [Abreu-Villaça et al., 2002](#); [Costa-Ferro et al., 2010](#)). The volume of the dissector (volume of interest, VOI) was obtained by multiplying the area of interest (AOI) by the dissector height. In our case, the dissector height corresponded to the slice height ([Costa-Ferro et al., 2010](#)).

Thus, in the VOIs, the neurons and glia cells were counted at different focal planes obtained during the course of focusing through the tissue slice. Neurons and glial cells found overlaying the left and upper borders of the VOI were counted together with the neurons and glial cells located within the analyzed VOI. Neurons and glial cells overlaying the right and lower border of VOI were not counted. Neuronal and glial densities were estimated using the following formula:  $D(est) = (1/ah) \times (PQ/PP)$ , where  $D(est)$  = estimated neuronal or glial densities;  $a$  = area (648.96  $\mu$ m<sup>2</sup>);  $h$  = dissector height (50  $\mu$ m);  $PQ$  = sum of neurons or glial cells counted;  $PP$  = sum of analyzed dissectors. The

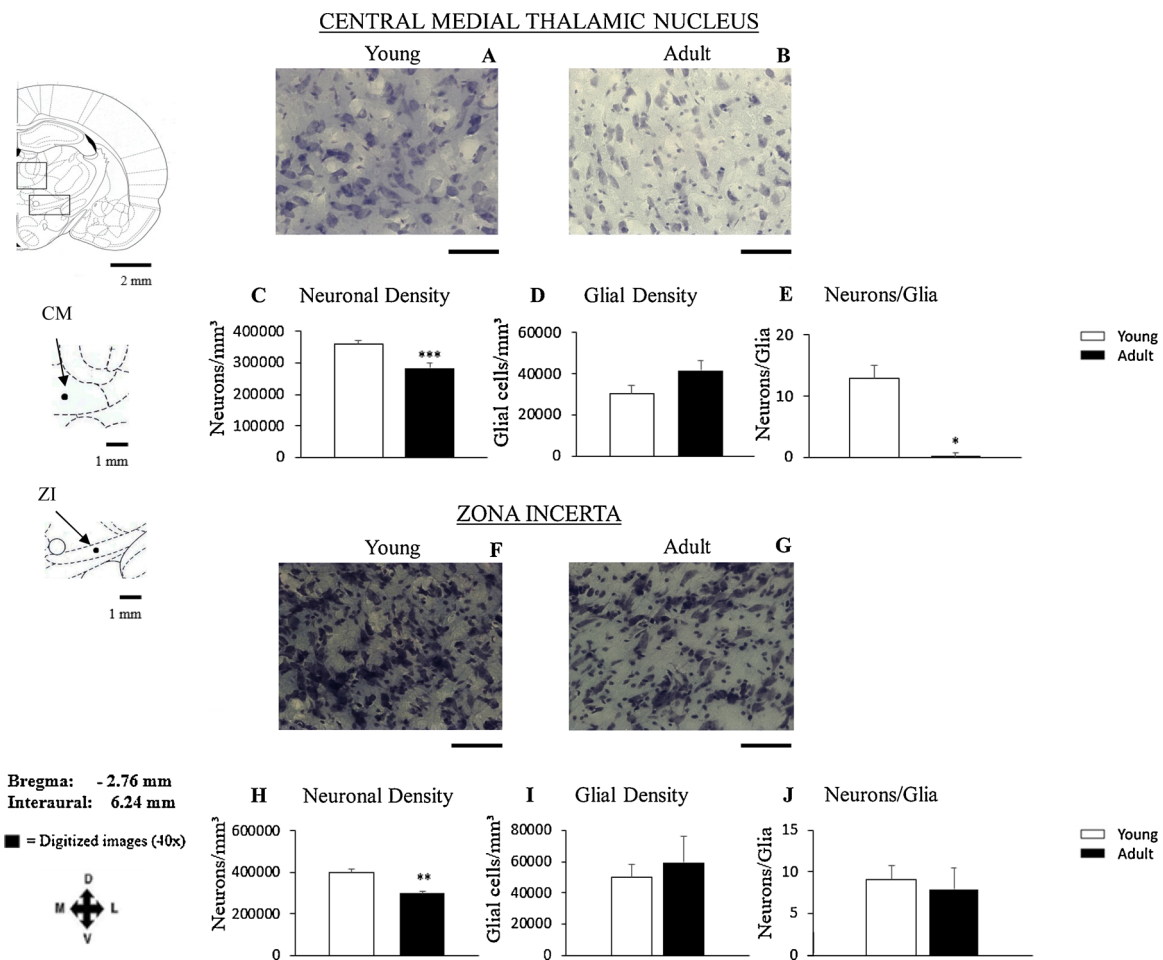


**Fig. 3.** Digitized images of coronal brain sections stained with Nissl showing the Central Medial Thalamic Nucleus (CM) (A, B, C, D, E) and Zona Incerta (ZI) (F, G, H, I, J) in young and mature adult male Wistar rats. The following parameters are presented: Neuronal density (neurons/mm<sup>3</sup>) (C, H) Glial Cell density (glia/mm<sup>3</sup>) (D, I) and Neuron/Glia ratio (Neuronal density/ Glial Cell density) (E, J). Note that only brain regions with significant morphological differences and/or relevant changes in GFAP immunoreactivity are presented in the figures, see Table 1. The schematic drawings were adapted from Paxinos and Watson's atlas (Paxinos and Watson, 2014) (Calibration bars = 100 μm) (\*\*P < 0.01; \*\*\*P < 0.001).

VOI size was set to count approximately five neurons and/or glial cells per VOI, to avoid errors related to the counting processes. The number of equidistant VOIs per region was defined in accordance with the brain region volume.

## 2.6. GFAP immunohistochemistry

To stain the GFAP, sections were collected in phosphate buffer saline solution (PBS, pH = 7.4) and processed following the unlabeled antibody peroxidase-antiperoxidase (PAP) procedure (Sternberger, 1979). Free floating sections were pretreated with 10% methanol in 3% H<sub>2</sub>O<sub>2</sub> for 30 min, then carefully washed and blocked with 2% bovine serum albumin (BSA) in PBS containing 0.4% Triton X-100 (PBSTx, Sigma Chemical Co., USA) for 30 min. They were then incubated with polyclonal GFAP antiserum raised in rabbit (Dako, UK) diluted 1:500 in PBS-Tx containing 2% BSA for 48 h at 4 °C. After being washed several times with PBS-Tx, the sections were incubated in PAP-conjugated anti-rabbit IgG (Amersham, UK) diluted 1:50 in PBS-Tx at room temperature for 2 h. The reaction was developed by first incubating the sections in a medium containing 0.06% 3,3'-diaminobenzidine (DAB, Sigma Chemical Co., USA) dissolved in PBS for 10 min and then, in the same solution containing 1 μL of 3% H<sub>2</sub>O<sub>2</sub> per mL of DAB medium for an additional 10 min. Finally, sections were rinsed in PBS, dehydrated in ethanol, cleared with xylene and covered with Permount and coverslips. Control sections were prepared omitting the primary antibody by

replacing it with PBS.

## 2.7. GFAP immunohistochemistry evaluation

The intensity of GFAP-immunoreactivity was measured using semi-quantitative densitometric analysis (Ferraz et al., 2003; Xavier et al., 2005; Martinez et al., 2006) using a BX 50 microscope (200 X; Olympus, Japan) coupled to a Motic Images Plus 2.0 camera and Image Pro Plus software (Image Pro-Plus 6.1, Media Cybernetics, Silver Spring, EUA). All lighting conditions and magnifications were kept constant during the process of capturing the images. Blood vessels and other artifacts were avoided, and the background correction was performed according to the procedure previously described (Xavier et al., 2005). The images were converted to an 8-bit gray scale (256 Gy levels) and areas of interest (AOIs) were overlaid the images (Saur et al., 2014).

To analyze astrocytic density and regional OD, AOIs measuring 6050 μm<sup>2</sup> were overlaid the studied images. To analyze the cellular OD, AOIs measuring 4.17 μm<sup>2</sup> were overlaid the astrocytic somata. The regional and cellular ODs were calculated according to the following formula (Martinez et al., 2006):

$$OD(x,y) = -\log [(INT(x,y) - BL)] / (INC - BL).$$

Where, OD(x,y) is the optical density at pixel (x,y), INT(x,y) is the intensity at pixel(x,y), BL or black is the intensity generated when no light

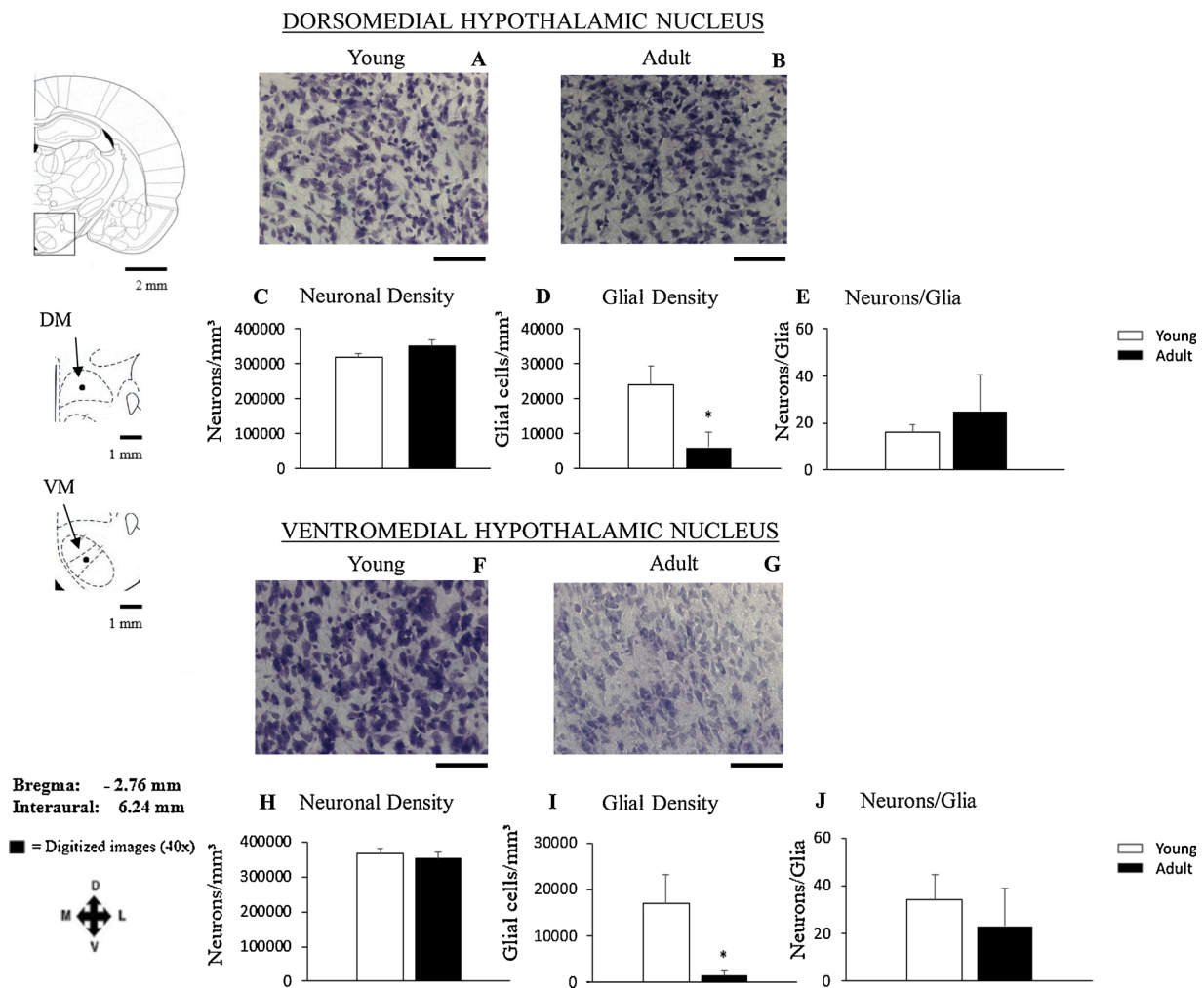


**Fig. 4.** Digitized images of coronal brain sections stained with Nissl showing the Dorsomedial Hypothalamic Nucleus (DM) (A, B, C, D, E) and Ventromedial Hypothalamic Nucleus (VM) (F, G, H, I, J) in young and mature adult male Wistar rats. The following parameters are presented: Neuronal density (neurons/mm<sup>3</sup>) (C, H) Glial Cell density (glia/mm<sup>3</sup>) (D, I) and Neuron/Glia ratio (Neuronal density/ Glial Cell density) (E, J). Note that only brain regions with significant morphological differences and/or relevant changes in GFAP immunoreactivity are presented in the figures, see Table 1. The schematic drawings were adapted from Paxinos and Watson's atlas (Paxinos and Watson, 2014) (Calibration bars = 100  $\mu$ m) (\*P < 0.05).

passes through the material and INC or incident is the intensity of the incident light.

To estimate GFAP-positive astrocytic density, the GFAP-positive astrocytes located inside this AOI or intersected by the upper and/or right edges of the square were counted. Astrocytes intersected by the lower and/or left edges of the square were not counted. The density of GFAP-positive astrocytes was calculated according to the following formula (Xavier et al., 2005):

$$Nv = \Sigma Q/a$$

Where,  $Nv$  is the estimated numerical density,  $\Sigma Q$  is the number of astrocytes counted in each AOI and the "a" is the AOI area.

### 2.8. Morphological analysis of astrocytes (Sholl Analysis)

An adaptation of Sholl's concentric circle method was performed using Image Pro Plus 6.0 software (Sholl, 1953; Dall'Oglio et al., 2008). This method consists of inserting virtual circles at intervals of 4.03  $\mu$ m around each astrocyte. The analyzed parameters were: 1- Primary process quantification, counting the processes extending directly from the astrocytic soma and 2- The degree of astrocytic ramification, evaluated by the number of intersections counted, i.e. counting the number of times the astrocytic processes intersected with each virtual circle

### 2.9. Statistical analysis

An unpaired Student's *t* test was used to compare young and mature adult rats,  $p < 0.05$ . Data for all variables is expressed as mean and standard deviation. The Graph Pad Prism software, version 7.03 was used in all the statistical analyses.

### 3. Results

As mentioned above, we chose to analyze the regions with more pronounced GFAP immunoreactivity located along the anterior-posterior axis in the middle of the brain. In this part of the brain, the following twelve regions presented more pronounced GFAP immunoreactivity in both, the young and mature adult Wistar rats: 1) Cerebral cortex (M1- primary motor cortex, M2- secondary motor cortex, S1Tr- primary somatosensory, trunk); 2) pyriform cortex; 3) dentate gyrus (granule cell layer); 4) corpus callosum; 5) CA1 hippocampus (stratum radiatum); 6) L.D.D.M; 7) L.D.V.L.; 8) habenula; 9) central medial thalamic nucleus; 10) zona incerta; 11) dorsomedial hypothalamic nucleus; and 12) ventromedial hypothalamic nucleus.

Quantitative analyzes of the Nissl stained sections showed decreased neuronal density in the mature adult group in the cerebral cortex ( $p < 0.001$ ), pyriform cortex ( $p < 0.001$ ) (Fig.1), L.D.D.M.

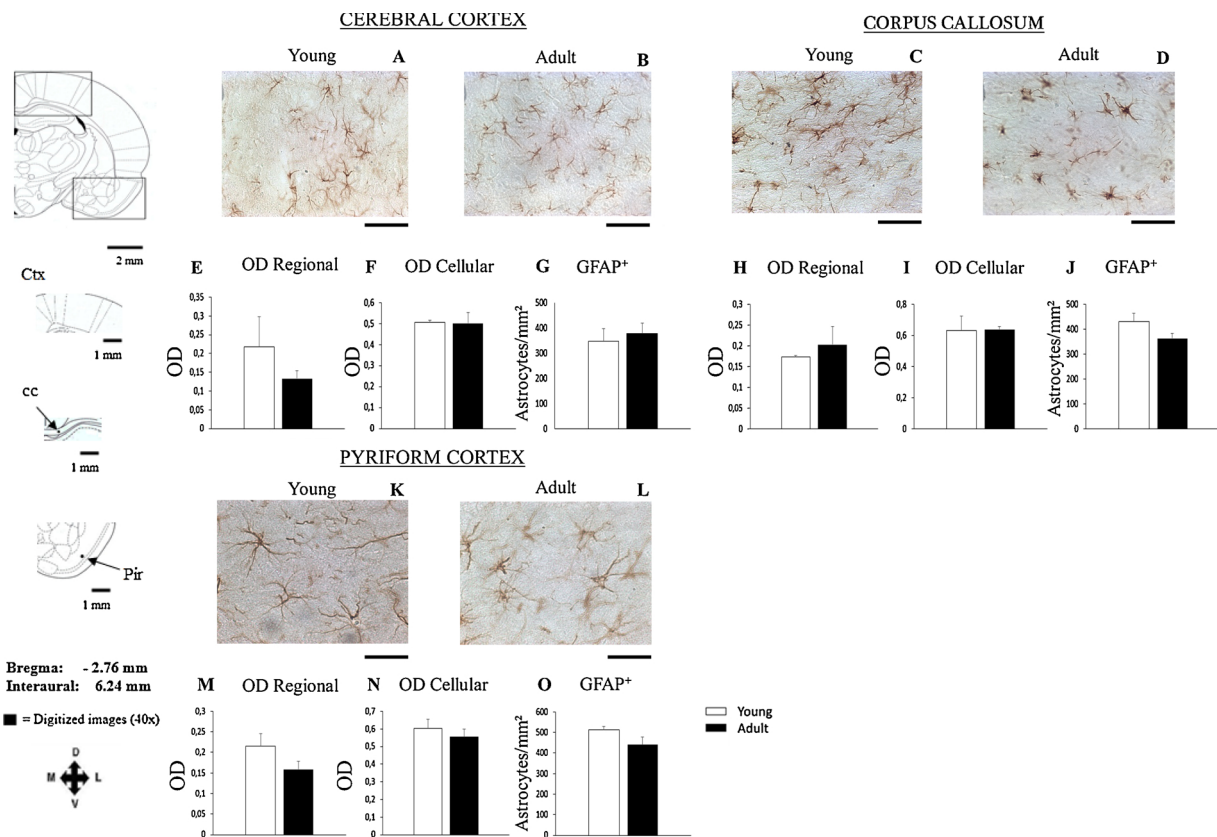


**Fig. 5.** Digitized images of coronal brain sections stained with GFAP immunohistochemistry showing the Cerebral cortex (Ctx) (A, B, E, F, G), Corpus Callosum (CC) (C, D, H, I, J) and Piriform Cortex (Pir) (K, L, M, N, O) in young and mature adult male Wistar rats. The following parameters are presented: GFAP-Regional optical density (OD Regional) (E, H, M), GFAP-Cellular optical density (OD Cellular) (F, I, N) and GFAP<sup>+</sup> Astrocytic density (GFAP<sup>+</sup> astrocytes/mm<sup>2</sup>) (GFAP<sup>+</sup>) (G, J, O). The schematic drawings were adapted from Paxinos and Watson's atlas (Paxinos and Watson, 2014) (Calibration bars = 100  $\mu$ m).

( $p < 0.05$ ), L.D.V.L. ( $p < 0.001$ ) (Fig. 2), central medial thalamic nucleus ( $p < 0.001$ ), *zona incerta* ( $p < 0.01$ ) (Fig. 3). Also, in the mature adult group, we observed decreases in glial density in corpus callosum ( $p < 0.05$ ) (Fig. 1), and in the dorsomedial and ventromedial hypothalamic nuclei ( $p < 0.05$ ) (Fig. 4). Despite these reductions, the neuron/glia ratio was increased in the habenula ( $p < 0.01$ ) (Fig. 2) and reduced in the central medial thalamic nucleus ( $p < 0.05$ ) (Fig. 3). No changes were observed in the neuronal or glial densities or in the neuron/glia ratio in either the dentate gyrus or hippocampus.

There were no changes in either the GFAP-positive astrocytic density or the GFAP-immunoreaction intensity, when mature adult animals were compared to young animals (Figs. 5–8). No significant differences were found in terms of the number of astrocytic primary processes or the degree of astrocytic ramification between young and mature animals in any of the studied regions. The Sholl analysis data is presented in Tables 1 and 2.

#### 4. Discussion

Our first important finding in this research showed the twelve brain regions which present the strongest GFAP immunoreaction, in male Wistar rats, during the period of life comprising young to mature adulthood. Similar results regarding GFAP distribution have been reported in previous studies (Kalman and Hajos, 1989; Zilles et al., 1991; Luo et al., 2017).

In our study, we observed a reduction in neuronal density in the cerebral cortex, piriform cortex, L.D.D.M, L.D.V.L, central medial thalamic nucleus and *zona incerta* in mature rats, revealing that neuronal loss until this period of life is confined to some brain regions.

No changes in neuronal density in the hypothalamic regions were

detected. However, apparently, this neuronal preservation is not a rule in all hypothalamic nuclei, since a previous study showed decreased neuronal density in the arcuate nucleus of male and female rodents, probably associated to decreases in gonadotrophin-releasing hormone (GnRH) during ageing (Sartin and Lamperti, 1985).

No changes in hippocampal (CA1 and CA3) neuronal or glial density were observed in our animals. Decreased hippocampal neuronal density has been described in mature and old rats of different ages - ranging between 12 and 24 months, (Mortera and Herculano-Houzel, 2012; Stranahan et al., 2012). The data on neuronal loss in humans is also controversial, some studies have reported neuronal loss in the CA1 subfield during aging (West and Gundersen, 1990; Šimić et al., 1997) while, another study reported no neuronal loss in the CA1 during normal aging (West et al., 1994).

No neurons were found in corpus callosum, only glial cells were observed in this region, it is a classic anatomical feature, previously described in other studies (Sturrock, 1976; Aboitiz and Montiel, 2003; Reyes-Haro et al., 2013). Those studies show that after postnatal-day 5, glial cells predominate in corpus callosum, representing 99% of all cells in this region (Sturrock, 1976; Aboitiz and Montiel, 2003; Reyes-Haro et al., 2013). In our study we found a decrease in glial density in the corpus callosum in mature animals. Few studies have investigated glial density in the corpus callosum during aging. Corroborating our findings, one classic study on this topic, involving young rats aged 0.75, 1, 1.5, 3.5 and 5 months, showed increased glial density in the corpus callosum in relation to the cortical neuron density from 0.75 to 3.5 months and a slight decrease in this ratio from 3.5 to 5 months (Ling and Leblond, 1973).

Other studies have described decreased neuronal density in Wistar rats aged between 12 and 24 months in the olfactory bulb, prefrontal

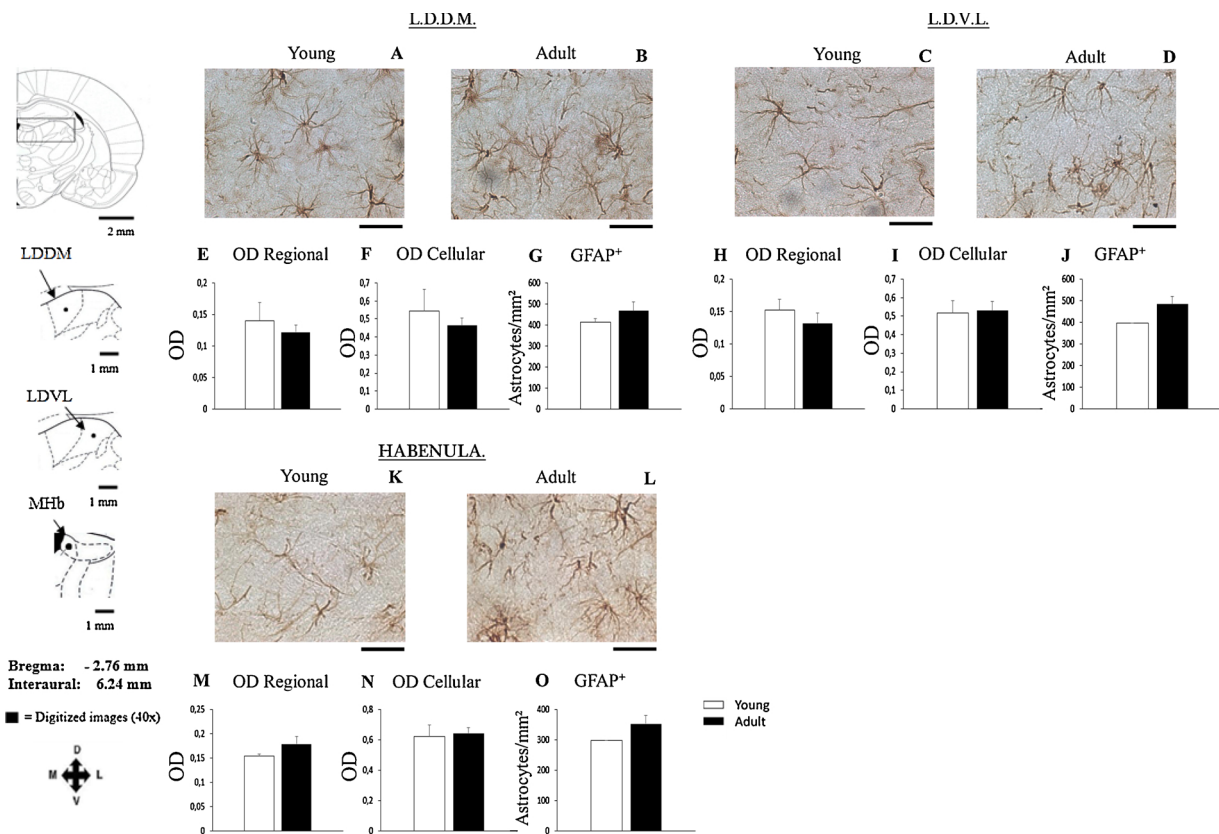


**Fig. 6.** Digitized images of coronal brain sections stained with GFAP immunohistochemistry showing the nucleus lateralis dorsale pars dorsomedialis (L.D.D.M.) (A, B, E, F, G), nucleus lateralis dorsale pars ventrolateralis (L.D.V.L.) (C, D, H, I, J) and Habenula (MHb) (K, L, M, N, O) in young and mature adult male Wistar rats. The following parameters are presented: GFAP-Regional optical density (OD Regional) (E, H, M), GFAP-Cellular optical density (OD Cellular) (F, I, N) and GFAP<sup>+</sup> Astrocytic density (GFAP<sup>+</sup> astrocytes/mm<sup>2</sup>) (GFAP<sup>+</sup>) (G, J, O). The schematic drawings were adapted from Paxinos and Watson's atlas (Paxinos and Watson, 2014) (Calibration bars = 100  $\mu$ m).

cortex and arcuate nucleus. Unfortunately, while these regions were not evaluated in our study, they can certainly be included in the “neuronal loss map” during the early stages of ageing (Mortera and Herculanou-Houzel, 2012; Stranahan et al., 2012; Sartin and Lamperti, 1985).

There were no changes to GFAP-positive astrocytic density or GFAP immunoreactivity. The data on GFAP during ageing is also controversial. A previous study reported that old (26-month-old) and very old (29-32-month-old) female Dawley rats present a decreased number of GFAP-positive astrocytes in the stratum radiatum, and these astrocytes have shortened processes and reduced branching complexity (Morel et al., 2015).

Another study found a similar reduction in GFAP activity in the entorhinal cortex of 24-month-old mice, mainly due to reduced astrocytic branching. The same study reported increased GFAP activity in the CA1 subfield and dentate gyrus (Rodriguez et al., 2014).

Another study showed that older mice (20–24 months) had 20% more GFAP-positive astrocytes than younger ones (3–4 months) in the dentate gyrus and CA1 subfield (Mouton et al., 2002). Additionally, several studies have shown that GFAP expression progressively increases during the later stages of aging in humans and rodents (Goss et al., 1991; Morgan et al., 1997, 1999; Nichols et al., 1993). In summary, these previous studies indicate that some specific brain regions present decreases while others present increases in GFAP activity during ageing. Qualitative and quantitative analyzes of our results show no changes in GFAP activity, suggesting changes in GFAP immunoreaction might only be significant after the early stages of aging.

We found that glial densities increased in cerebral cortex and decreased in dorsomedial hypothalamic nucleus in mature adults. These changes were unassociated with changes in GFAP immunoreactivity. In fact, GFAP positive astrocytes represent a portion of the total astrocytes,

and consequently a subpopulation of glial cells found in the brain. These changes in the glial population may have occurred in the non-GFAP positive astrocytes or other glial cells, like microglia and/or oligodendrocytes (Vaughan and Peters, 1974; Xiaoli et al., 2006). An interesting issue for future studies could be to evaluate astrocytes, microglia and oligodendrocytes in those areas during aging using different immunostaining techniques such as CNPase (oligodendrocyte marker) and isolectin B4 (microglial cells marker) that are able to mark different glial cell types (Hayakawa et al., 2007).

GFAP immunohistochemistry only labels the astrocytic subpopulation, while other markers, including S100 protein, vimentin and glutamine synthetase can also be used to analyze glial cells (Catalani et al., 2002). To the best of our knowledge, GFAP represents the most reliable and widely used marker for in vivo and in vitro identification of astrocytes and has been used as the main marker for astrocytic reactivity in several studies (Bignami et al., 1972; Bignami and Dahl, 1977; Kalman and Hajos, 1989; Zilles et al., 1991; Kohama et al., 1995; Nichols, 1999; Cotrina and Nedergaard, 2002; Theodosios et al., 2008; Middeldorp and Hol, 2011; Schafer et al., 2012; Saur et al., 2014; Salazar et al., 2014; Luo et al., 2017). When compared to GFAP, the other markers present some serious disadvantages. For example, antibodies for glutamine synthetase and S100b were found to clearly stain the nuclei of astrocytes, while the cytoplasm and processes were only poorly stained (Wu et al., 2005). Using S100b immunohistochemistry, the astrocytic processes appear to be smaller when compared to GFAP immunolabeled astrocytes (Björklund et al., 1983). Moreover, glutamine synthetase is also detectable in oligodendrocytes (Tansey et al., 1991). Vimentin is also a good marker of astrocytic morphology, but it is predominantly expressed in immature glial cells (Dahl et al., 1981; Pixley and Vellis, 1984), and in our study, we focused on the effects of

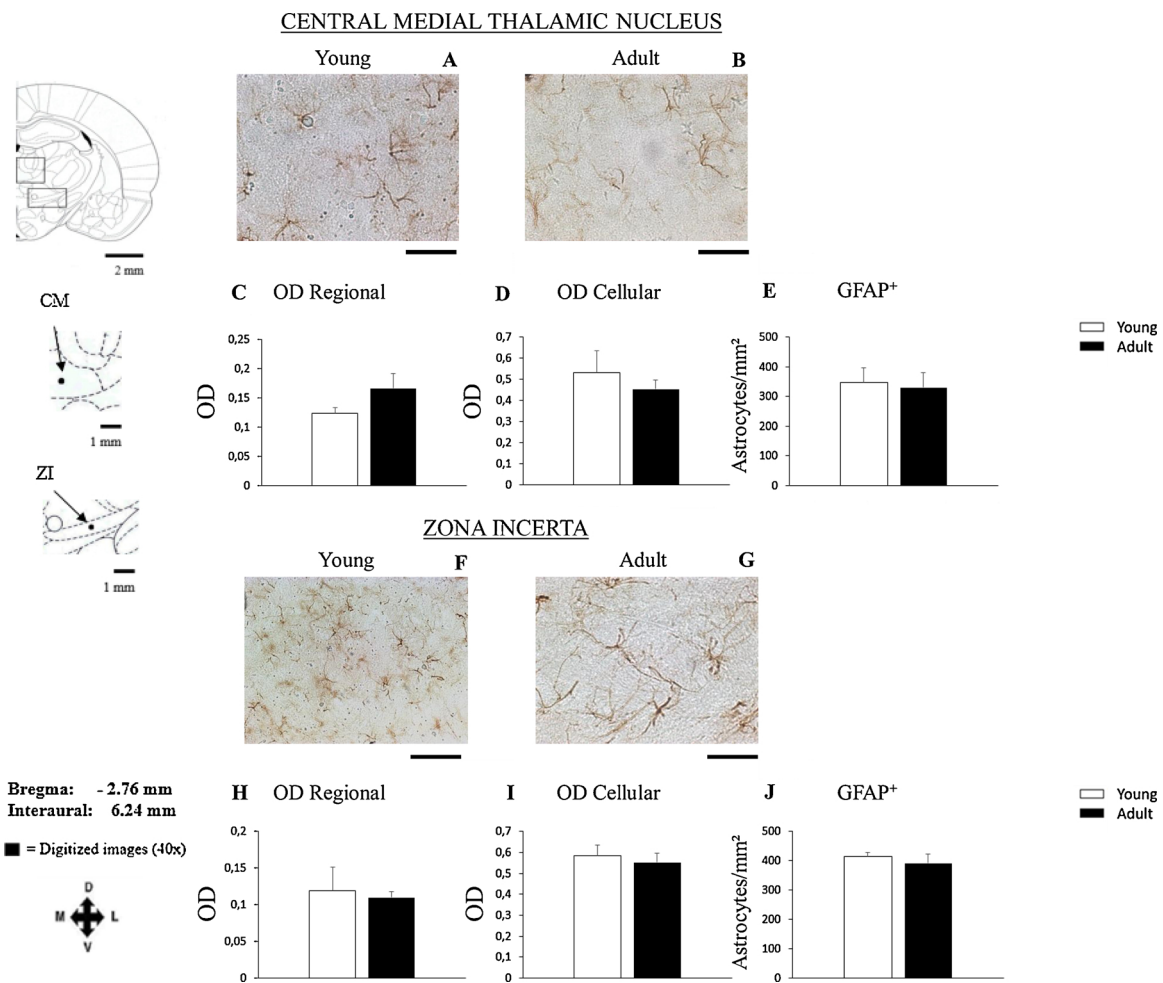


**Fig. 7.** Digitized images of coronal brain sections stained with GFAP immunohistochemistry showing the Central Medial Thalamic Nucleus (CM) (A, B, C, D, E) and Zona Incerta (ZI) (F, G, H, I, J) in young and mature adult male Wistar rats. The following parameters are presented: GFAP-Regional optical density (OD Regional) (C, H), GFAP-Cellular optical density (OD Cellular) (D, I) and GFAP<sup>+</sup> Astrocytic density (GFAP<sup>+</sup> astrocytes/mm<sup>2</sup>) (GFAP<sup>+</sup>) (E, J). The schematic drawings were adapted from Paxinos and Watson's atlas (Paxinos and Watson, 2014) (Calibration bars = 100  $\mu$ m).

natural ageing on the structure and function of developed astrocytes. Additionally, several morphometrical parameters may be evaluated using GFAP, such as: astrocytic density, regional and cellular optical density and the degree of ramification using the concentric Sholl circle technique. Therefore, GFAP immunohistochemistry presents more reliable results when compared with other immunohistochemical markers. Future studies, using other previously cited techniques might produce important complementary data to our findings.

The pattern of astrocytic ramification may undergo changes in either beneficial situations such as environmental enrichment (Viola et al., 2009; Sampedro-Piquero et al., 2014) and physical exercise (Saur et al., 2014) or in negative situations, such as stroke (Mestriner et al., 2015) and psychiatric diseases like depression (Kraig et al., 1991). The initial phase of natural ageing, typically free of comorbidities, may not provoke perceptible morphological changes in astrocytic ramification, since no differences were detected regarding the degree of astrocytic ramification when comparing young and mature adult animals

In our study we analyze the brains of 14 month-old rats, (mature rats) to evaluate the first steps in brain aging. Many reliable and unbiased studies have analyzed the neuronal and glial populations in very aged rats, using stereological tools and other morphological methods (Hsu and Peng, 1978; Sabel and Stein, 1981; Sartin and Lamperti, 1985;

Hayakawa et al., 2007; Chen et al., 2011; Morterá and Herculano-Houzel, 2012; Stranahan et al., 2012; Fiuza et al., 2017). However, few studies have analyzed mature rats, thus, future studies, again using middle-aged rodents, could improve the knowledge regarding this initial phase of aging.

In summary, our study provides new data on neuronal and glial densities and GFAP immunoreactivity in different brain regions of 45-day-old and 420-day-old Wistar rats. We hope our study will be useful to other researchers attempting to understand the neurobiology of this so relevant animal model during this period of life.

## 5. Conclusions

In conclusion, our data show that in Wistar rats: 1- Some brain regions are more susceptible to neuronal and glial loss during this period of life, while other regions show no reduction; 2- The normal ageing process is not associated with changes in GFAP immunoreaction in the studied brain regions prior to the mature adult stage.

Our study provides new information about brain morphology and GFAP activity in mature male Wistar rats, which sheds light on the neurobiology of this animal model in this important period of life.

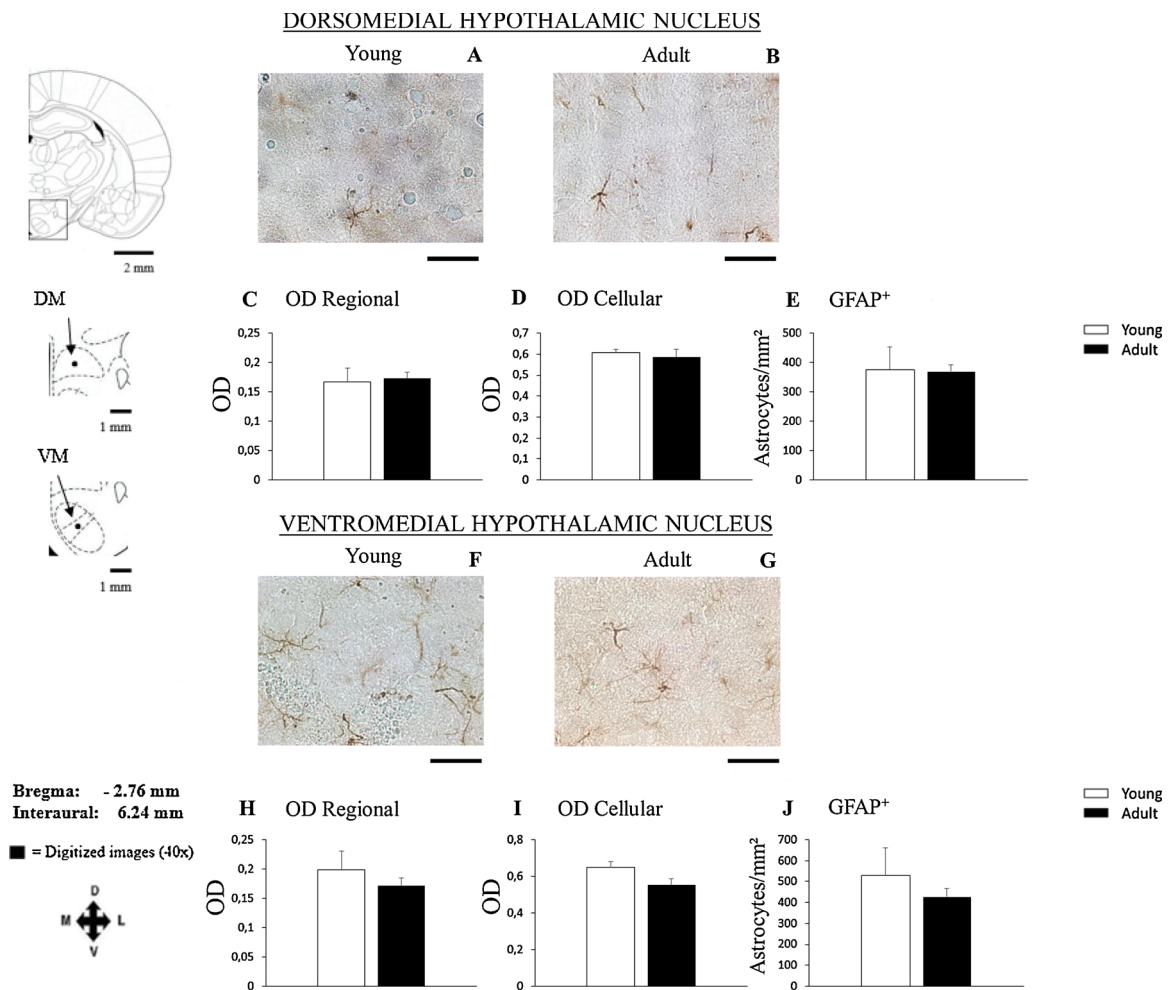


**Fig. 8.** Digitized images of coronal brain sections stained with GFAP immunohistochemistry showing the Dorsomedial Hypothalamic Nucleus (DM) (A, B, C, D, E) and Ventromedial Hypothalamic Nucleus (VM) (F, G, H, I, J) in young and mature adult male Wistar rats. The following parameters are presented: GFAP-Regional optical density (OD Regional) (C, H), GFAP-Cellular optical density (OD Cellular) (D, I) and GFAP<sup>+</sup> Astrocytic density (GFAP<sup>+</sup> astrocytes/mm<sup>2</sup>) (GFAP<sup>+</sup>) (E, J). The schematic drawings were adapted from Paxinos and Watson's atlas (Paxinos and Watson, 2014) (Calibration bars = 100 μm).

**Table 1**

Summary of data obtained from the Sholl's analysis: Number of Primary Processes/GFAP + Astrocytes and Number of Intersections/GFAP + Astrocytes (Degree of Ramification).

Brain region	Number of Astrocytes Primary Processes					Number of Intersections/GFAP + Astrocytes (Degree of Ramification)				
	Young		Mature adult		P-value	Young		Mature adult		P-value
	Mean	SD	Mean	SD		Mean	SD	Mean	SD	
Cerebral Cortex	2.85	0.63	3.90	0.52	0.09	8.15	1.20	15.77	6.81	0.21
Corpus Callosum	2.85	0.21	3.35	0.30	0.10	8.90	0.98	9.30	1.25	0.71
Pyriiform Cortex	2.95	0.35	3.88	0.58	0.11	11.00	2.12	18.70	3.75	0.06
L.D.D.M.	3.20	0.14	3.30	0.18	0.54	12.40	0.56	11.55	3.24	0.74
L.D.V.L.	3.00	0.01	3.30	0.33	0.38	9.75	0.91	13.50	5.58	0.42
Habenula	2.70	0.01	3.10	0.31	0.17	7.40	0.84	9.77	2.38	0.26
Central Medial Thalamic Nucleus	2.80	0.01	3.55	0.85	0.30	7.95	1.20	11.01	2.89	0.24
Zona Incerta	3.10	0.01	3.06	0.25	0.85	9.55	0.77	10.4	2.46	0.68
Dorsomedial Hypothalamic Nucleus	3.25	0.17	3.16	1.60	0.74	9.75	1.94	10.93	5.81	0.60
Ventromedial Hypothalamic Nucleus	3.17	0.17	3.61	1.84	0.29	10.75	1.76	14.16	7.44	0.23

**Table 2**

Summary of our quantitative analysis: Neuronal density (neurons/mm<sup>3</sup>), Glial density (glia/mm<sup>3</sup>), Neuron/glia ratio (Neuronal density/ Glial Cell density); semi-quantitative analysis (GFAP- Regional optical density and GFAP-cellular optical density), GFAP<sup>+</sup> density (number of GFAP<sup>+</sup> astrocytes/ mm<sup>2</sup>), Astrocytic Primary Processes and degree of astrocytic Ramification in young and mature adult male Wistar rats. The findings in the mature adult group in relation to the young group are represented by arrows, ↑ Increase; ↓ Decrease; = no change; - not performed; ↓ (p < 0.05); ↑↑ (p < 0.01) and ↓↓↓ (p < 0.001).

		Neuronal Density	Glial Density	Neurons/Glia	GFAP Regional	OD -	GFAP OD - Cellular	GFAP+ Density	Astrocytes Primary Processes	Astrocytes Degree of Ramification
TELENCEPHALON	Cerebral Cortex	↓↓↓	-	-	-	-	-	-	-	-
	Pyriform Cortex	↓↓↓	-	-	-	-	-	-	-	-
	Dentate Gyrus	-	-	-	-	-	-	-	-	-
	Corpus Callosum	-	↓	-	-	-	-	-	-	-
THALAMUS	Habenula	-	-	↑↑	-	-	-	-	-	-
	Central Medial Thalamic Nucleus	↓↓↓	-	↓	-	-	-	-	-	-
	L.D.D.M.	↓	-	-	-	-	-	-	-	-
	L.D.V.L.	↓↓↓	-	-	-	-	-	-	-	-
	Uncertain Zone	↓↓↓	-	-	-	-	-	-	-	-
HYPOTHALAMUS	Dorsomedial Hypothalamic Nucleus	-	↓	-	-	-	-	-	-	-
	Ventromedial Hypothalamic Nucleus	-	↓	-	-	-	-	-	-	-

## Acknowledgements

This study was financed by the Coordenação de Aperfeiçoamento de Pessoal de Nível Superior – Brasil (CAPES) – Finance Code 001, Conselho Nacional de Pesquisa e Desenvolvimento (CNPq) (Grant number 3066442016-9) and Fundação de Amparo à Pesquisa do Estado do Rio Grande do Sul (FAPERGS). JCC and LLX are CNPq investigators.

## References

Abotiz, F., Montiel, J., 2003. One hundred million years of interhemispheric communication: the history of the corpus callosum. *Braz. J. Med. Biol. Res.* 36, 409–420.

Abreu-Villaça, Silva W.C., Manhães, A.C., Schmidt, S.L., 2002. The effect of corpus callosum agenesis on neocortical thickness and neuronal density of BALB/cCF mice. *Brain Res. Bull.* 58, 411–416.

Andreollo, N.A., Santos, E.F., Araújo, M.R., Lopes, L.R., 2012. Rat's age versus human's age: what is the relationship? *Arq. Bras. Cir. Dig.* 25 (1), 49–51.

Bellaver, B., Souza, D.G., Souza, D.O., Quincozes-Santos, A., 2016. Hippocampal astrocyte cultures from adult and aged rats reproduce changes in glial functionality observed in the aging brain. *Mol. Neurobiol.* 1–17.

Bignami, A., Dahl, D., 1977. Specificity of the glial fibrillary acidic protein for astroglia. *J. Histochem. Cytochem.* 25, 466–469.

Bignami, B.A., Eng, L.F., Dahl, D., Uyeda, C.T., 1972. Localization of the glial fibrillary acidic protein isolated from fibrous astrocytes. *Brain Res.* 43, 429–435.

Björklund, H., Dahl, D., Haglid, K., Rosengren, L., Olson, L., 1983. Astrocytic development in fetal parietal cortex grafted to cerebral and cerebellar cortex of immature rats. *Brain Res.* 285 (2), 171–180.

Catalani, et al., 2002. Glial fibrillary acidic protein immunoreactive astrocytes in developing rat hippocampus. *Mech. Ageing Dev.* 123 (5), 481–490.

Chen, L., Lu, W., Yang, Z., Yang, S., Li, C., Shi, X., Tang, Y., 2011. Age-related changes of the oligodendrocytes in rat subcortical white matter. *Anat. Rec. Adv. Integr. Anat. Evol. Biol.* 294 (3), 487–493.

Chinta, S.J., Lieu, C.A., DeMaria, M., Laberge, R.M., Campisi, J., Andersen, J.K., 2014. Environmental stress, ageing and glial cell senescence: a novel mechanistic link to Parkinson's disease? *Natl. Inst. Health* 273 (5), 429–436.

Chung, H.Y., Cesari, M., Anton, S., Marzetti, E., Giovannini, S., Seo, A.Y., et al., 2009. Molecular inflammation: underpinnings of aging and age-related diseases. *Ageing Res. Rev.* 8, 18–30.

Costa-Ferre, Z.S.M., Vitola, A.S., Pedrosa, M.F., Cunha, F.B., Xavier, L.L., Machado, D.C., et al., 2010. Prevention of seizures and reorganization of hippocampal functions by transplantation of bone marrow cells in the acute phase of experimental epilepsy. *Seizure* 19, 84–92.

Cotrina, M.L., Nedergaard, M., 2002. Astrocytes in the aging brain. *J. Neurosci. Res.* 67, 1–10.

Dahl, et al., 1981. Vimentin, the 57 000 molecular weight protein of fibroblast filaments, is the major cytoskeletal component in immature glia. *Eur. J. Cell Biol.* 24 (2),

191–196.

Dall'Oglio, A., Gehlen, G., Achaval, M., Rasia-Filho, A.A., 2008. Dendritic branching features of Golgi-impregnated neurons from the “ventral” medial amygdala subnuclei of adult male and female rats. *Neurosci. Lett.* 439, 287–292.

Eddleston, M., Mucke, L., 1993. Molecular profile of reactive astrocytes—implications for their role in neurologic disease. *Neuroscience* 54, 15–36.

Eng, L.F., Yu, A.C., Lee, Y.L., 1992. Astrocytic response to injury. *Prog. Brain Res.* 94, 353–365.

Fabricius, K., Jacobsen, J.S., Pakkenberg, B., 2013. Effect of age on neocortical brain cells in 90+ year old human females—a cell counting study. *Neurobiol. Ageing* 34, 91–99.

Ferraz, A.C., Xavier, L.L., Hernandez, S., Sulzbach, M., Viola, G.G., Anselmo-Franci, J.A., et al., 2003. Failure of estrogen to protect the substantia nigra pars compacta of female rats from lesion induced by 6-hydroxydopamine. *Brain Res.* 986, 200–205.

Fiuza, F.P., et al., 2017. Region-specific glial hyperplasia and neuronal stability of rat lateral geniculate nucleus during aging. *Exp. Gerontol.* 100, 91–99.

Giaume, C., Kirchoff, F., Matute, C., Reichenbach, A., Verkhratsky, A., 2007. Glia: the fulcrum of brain diseases. *Cell Death Differ.* 14, 1324e1335.

Gomes, F.C.A., Tortelli, V.P., Diniz, L., 2013. Glia: dos velhos conceitos às novas funções de hoje e as que ainda virão. *Estud. av. São Paulo* 27 (77), 61–84.

Goss, J.R., Finch, C.E., Morgan, D.G., 1991. Age-related changes in glial fibrillary acidic protein mRNA in the mouse brain. *Neurobiol. Ageing* 12 (2), 165–170.

Hayakawa, N., Kato, H., Araki, T., 2007. Age-related changes of astrocytes, oligodendrocytes and microglia in the mouse hippocampal CA1 sector. *Mech. Ageing Dev.* 128 (4), 311–316.

Hsu, H.K., Peng, M.T., 1978. Hypothalamic neuron number of old female rats. *Gerontology* 24 (6), 434–440.

Jyothia, H.J., Vidyadhara, D.J., Mahadevan, A., Philip, M., Parmar, S.K., Gowri, M.S., et al., 2015. Aging causes morphological alterations in astrocytes and microglia in human substantia nigra pars compacta. *Neurobiol. Ageing* 36, 3321–3333.

Kalia, L.V., Lang, A.E., 2015. Parkinson's disease. *Lancet* 386, 896–912.

Kalman, M., Hajos, F., 1989. Distribution of glial fibrillary acidic protein (GFAP)-immunoreactive astrocytes in the rat brain. *Exp. Brain Res.* 78 (1), 147–163.

Kohama, S.G., Goss, J.R., Finch, C.E., McNeill, T.H., 1995. Increases of glial fibrillary acidic protein in the aging female mouse brain. *Neurobiol. Ageing* 16, 59–67.

Kraig, R.P., Dong, L., Thisted, R., Jaeger, C.B., 1991. Spreading depression increases immunohistochemical staining of glial fibrillary acidic protein. *J. Neurosci.* 17 (7), 2187–2199.

Ling, E.A., Leblond, C.P., 1973. Investigation of glial cells in semithin sections. II. Variation with age in the numbers of the various glial cell types in rat cortex and corpus callosum. *J. Comp. Neurol.* 149 (1), 73–81.

Lopez-Leon, M., Reggiani, P.C., Herenu, C.B., Goya, R.G., 2014. Regenerative medicine for the aging brain. *Environ. Health Perspect.* 122 (1), 1–9.

Luo, H., Wu, X.Q., Zhao, M., Wang, Q., Jiang, G.P., Cai, W.J., Luo, M.Y., 2017. Expression of vimentin and glial fibrillary acidic protein in central nervous system development of rats. *Asian Pac. J. Trop. Med.* 10 (12), 1185–1189.

Lynch, A.M., Murphy, K.J., Deighan, B.F., O'Reilly, J.A., Gun'ko, Y.K., Cowley, T.R., et al., 2010. The impact of glial activation in the aging brain. *Ageing Dis.* 1, 262–278.

Martinez, F.G., Hermel, E.E., Xavier, L.L., Viola, G.G., Riboldi, J., Rasia-Filho, A.A., et al., 2006. Gonadal hormone regulation of glial fibrillary acidic protein immunoreactivity

- in the medial amygdala subnuclei across the estrous cycle and in castrated and treated female rats. *Brain Res.* 1108, 117–126.
- Menet, V., y Ribotta, M.G., Chauvet, N., Drian, M.J., Lannoy, J., Colucci-Guyon, E., et al., 2001. Inactivation of the glial fibrillary acidic protein gene, but not that of vimentin, improves neuronal survival and neurite growth by modifying adhesion molecule expression. *J. Neurosci.* 21, 6147–6158.
- Mestriner, R.G., Saur, L., Bagatini, P.B., Baptista, P.P.A., Vaz, S.P., Xavier, L.L., et al., 2015. Astrocyte morphology after ischemic and hemorrhagic experimental stroke has no influence on the different recovery patterns. *Behav. Brain Res.* 278, 257–261.
- Middeldorp, J., Hol, E.M., 2011. GFAP in health and disease. *Prog. Neurobiol.* 93 (3), 421–443.
- Morel, G.R., Andersen, T., Pardo, J., Zuccolilli, G.O., Cambiaggi, V., Hereñú, C.B., Goya, R.G., 2015. Cognitive impairment and morphological changes in the dorsal hippocampus of very old female rats. *Neuroscience* 303, 189–199.
- Morgan, T.E., Rozovsky, I., Goldsmith, S.K., Stone, D.J., Yoshida, T., Finch, C.E., 1997. Increased transcription of the astrocyte gene GFAP during middle-age is attenuated by food restriction: implications for the role of oxidative stress. *Free Radic. Biol. Med.* 23 (3), 524–528.
- Morgan, T.E., Xie, Z., Goldsmith, S., Yoshida, T., Lanzrein, A.S., Stone, D., et al., 1999. The mosaic of brain glial hyperactivity during normal ageing and its attenuation by food restriction. *Neuroscience* 89 (3), 687–699.
- Mortera, P., Herculano-Houzel, S., 2012. Age-related neuronal loss in the rat brain starts at the end of adolescence. *Front. Neuroanat.* 6, 1–9.
- Mouton, P.R., Long, J.M., Lei, D.L., Howard, V., Jucker, M., Calhoun, M.E., et al., 2002. Age and gender effects on microglia and astrocyte numbers in brains of mice. *Brain Res.* 956 (1), 30–35.
- Mythri, R.B., Venkateshappa, C., Harish, G., Mahadevan, A., Muthane, U.B., Yasha, T.C., et al., 2011. Evaluation of markers of oxidative stress, antioxidant function and astrocytic proliferation in the striatum and frontal cortex of Parkinson's disease brains. *Neurochem. Res.* 36, 1452–1463.
- Nichols, N.R., 1999. Glial responses to steroids as markers of brain aging. *J. Neurobiol.* 40, 585e601.
- Nichols, N.R., Day, J.R., Laping, N.J., Johnson, S.A., Finch, C.E., 1993. GFAP mRNA increases with age in rat and human brain. *Neurobiol. Aging* 14 (5), 421–429.
- Ojo, J.O., Rezaie, P., Gabbott, P.L., Stewart, M.G., 2015. Impact of age related neuroglial cell responses on hippocampal deterioration. *Front. Aging Neurosci.* 7, 57.
- Paxinos, G., Watson, C., 2014. *The Rat Brain in Stereotaxic Coordinates*, 7th edition. Elsevier Academic Press, New York, pp. 472.
- Pekny, M., Pekna, M., 2004. Astrocyte intermediate filaments in CNS pathologies and regeneration. *J. Pathol.* 204 (November (4)), 428–437.
- Pixley, S.K., Vellis, J., 1984. Transition between immature radial glia and mature astrocytes studied with a monoclonal antibody to vimentin. *Dev. Brain Res.* 15 (2), 201–209.
- Reyes-Haro, D., Mora-Loyola, E., Soria-Ortiz, B., Garcia-Colunga, J., 2013. Regional density of glial cells in the rat corpus callosum. *Biol. Res.* 46 (1), 27–32.
- Rodríguez, J.J., Olabarria, M., Chvatal, A., Verkhatsky, A., 2009. Astroglia in dementia and Alzheimer's disease. *Cell Death Differ.* 16, 378–385.
- Rodríguez, J.J., Terzieva, S., Olabarria, M., Lanza, R.G., Verkhatsky, A., 2013. Enriched environment and physical activity reverse astroglial degeneration in the hippocampus of AD transgenic mice. *Cell Death Dis.* 4, e678.
- Rodríguez, J.J., Yeh, C.Y., Terzieva, S., Olabarria, M., Kulijewicz-Nawrot, M., Verkhatsky, A., 2014. Complex and region-specific changes in astroglial markers in the aging brain. *Neurobiol. Aging* 35, 15–23.
- Rodríguez-Arellano, J.J., Parpura, V., Zorec, R., Verkhatsky, A., 2016. Astrocytes in physiological aging and Alzheimer's disease. *Neuroscience* 323, 170–182.
- Sabel, B.A., Stein, D.G., 1981. Extensive loss of subcortical neurons in the aging rat brain. *Exp. Neurol.* 73 (2), 507–516.
- Salazar, A.P., Quagliotto, E., Alves, J., SAUR, L., XAVIER, L.L., et al., 2014. Effect of prior exercise training and myocardial infarction-induced heart failure on the neuronal and glial densities and the GFAP-immunoreactivity in the posterodorsal medial amygdala of rats. *Histol. Histopathol.* 29, 1423–1435.
- Sampedro-Piquero, P., De Bartolo, P., Petrosini, L., Zancada-Menendez, C., Arias, J.L., Begega, A., 2014. Astrocytic plasticity as a possible mediator of the cognitive improvements after environmental enrichment in aged rats. *Neurobiol. Learn. Mem.* 114, 16–25.
- Sartin, J.L., Lamperti, A.A., 1985. Neuron numbers in hypothalamic nuclei of young, middle-aged and aged male rats. *Experientia* 41, 109–111.
- Saur, L., Baptista, P.P., de Senna, P.N., Paim, M.F., do Nascimento, P., Ilha, J., et al., 2014. Physical exercise increases GFAP expression and induces morphological changes in hippocampal astrocytes. *Brain Struct. Funct.* 219, 293–302.
- Schafer, S., Calas, A.G., Vergouts, M., Hermans, E., 2012. Immunomodulatory influence of bone marrow derived mesenchymal stem cells on neuroinflammation in astrocyte cultures. *J. Neuroimmunol.* 249 (1–2), 40–48.
- Seifert, G., Schilling, K., Steinhäuser, C., 2006. Astrocyte dysfunction in neurological disorders: a molecular perspective. *Nat. Rev. Neurosci.* 7, 194–206.
- Sengupta, P., 2013. The laboratory rat: relating its age with human's. *Int. J. Prev. Med.* 4 (6), 624–630.
- Sholl, D.A., 1953. Dendritic organization in the neurons of the visual and motor cortices of the cat. *J. Anat.* 87, 387–406.
- Šimić, G., Kostović, I., Winblad, B., Bogdanović, N., 1997. Volume and number of neurons of the human hippocampal formation in normal aging and Alzheimer's disease. *J. Comp. Neurol.* 379 (4), 482–494.
- Sofroniew, M.V., 2009. Molecular dissection of reactive astroglia and glial scar formation. *Trends Neurosci.* 32, 638–647.
- Sofroniew, M.V., Vinters, H.V., 2010. Astrocytes: biology and pathology. *Acta Neuropathol.* 119, 7–35.
- Stereo, D.C., 1984. The unbiased estimation of number and sizes of arbitrary particles using the disector. *J. Microsc.* 1, 127–136.
- Sternberger, L.A., 1979. The unlabeled antibody (PAP) method, introduction. *J. Histochem. Cytochem.* 27, 1657.
- Stranahan, A.M., Jiam, N.T., Spiegel, A.M., Gallagher, M., et al., 2012. Aging reduces total neuron number in the dorsal component of the rodent prefrontal cortex. *J. Comp. Neurol.* 520 (6), 1318–1326.
- Sturrock, R.R., 1976. Light microscopic identification of immature glial cells in semithin sections of the developing mouse corpus callosum. *J. Anat.* 122, 521–537.
- Tansey, F.A., Farooq, M., Cammer, W., 1991. Glutamine synthetase in oligodendrocytes and astrocytes: new biochemical and immunocytochemical evidence. *J. Neurochem.* 56 (1), 266–272.
- Tansey, M.G., Goldberg, M.S., 2010. Neuroinflammation in Parkinson's disease: its role in neuronal death and implications for therapeutic intervention. *Neurobiol. Dis.* 37 (3), 510–518.
- Theodosios, T.D., Dominique, A., Poulain, D.A., Oliet, S.H.R., 2008. Activity dependent structural and functional plasticity of astrocyte neuron interactions. *Physiol. Rev.* 88 (3), 983–1008.
- Unger, J.W., 1998. Glial reaction in aging and Alzheimer's disease. *Microsc. Res. Tech.* 43, 24–28.
- Vaughan, D.W., Peters, A., 1974. Neuroglial cells in the cerebral cortex of rats from young adulthood to old age: an electron microscope study. *J. Neurocytol.* 3, 405–429.
- Verkhatsky, A., Sofroniew, M.V., Messing, A., deLanerolle, N.C., Rempe, D., Rodríguez, J.J., et al., 2012. Neurological diseases as primary gliopathies: a reassessment of neurocentrism. *ASN Neuro* 4, e00082.
- Viola, G.G., Rodrigues, L., Américo, J.C., Hansel, G., Vargas, R.S., Xavier, L.L., et al., 2009. Morphological changes in hippocampal astrocytes induced by environmental enrichment in mice. *Brain Res.* 1274, 47–54.
- West, M.J., Gundersen, H.J.G., 1990. Unbiased stereological estimation of the number of neurons in the human hippocampus. *J. Comp. Neurol.* 296 (1), 1–22.
- West, M.J., Coleman, P.D., Flood, D.G., Troncoso, J.C., 1994. Differences in the pattern of hippocampal neuronal loss in normal ageing and Alzheimer's disease. *Lancet* 344 (8925), 769–772.
- Wu, Y., Zhang, A., Yew, D.T., 2005. Age related changes of various markers of astrocytes in senescence-accelerated mice hippocampus. *Neurochem. Int.* 46, 565–574.
- Xavier, L.L., Viola, G.G., Ferraz, A.C., da Cunha, C., Deonizio, J.M., Netto, C.A., Achaval, M., 2005. A simple and fast densitometric method for the analysis of tyrosine hydroxylase immunoreactivity in the substantia nigra pars compacta and in the ventral tegmental area. *Brain Res. Protoc.* 16, 58–64.
- Xiaoli, W., Yun, X., Fang, W., Lihua, T., Zhilong, L., Honglian, L., Shenghong, L., 2006. Aging related changes of microglia and astrocytes in hypothalamus after intraperitoneal injection of hypertonic saline in rats. *J. Huazhong Univ. Sci. Technol. [Med. Sci.]* 26 (2), 231–234.
- Zilles, K., Hajós, F., Kálmán, M., Schleicher, A., 1991. Mapping of glial fibrillary acidic protein-immunoreactivity in the rat forebrain and mesencephalon by computerized image analysis. *J. Comp. Neurol.* 308 (3), 340–355.